

CINESCENE: Implicit 3D as Effective Scene Representation for Cinematic Video Generation

Kaiyi Huang^{1*} Yukun Huang¹ Yu Li³ Jianhong Bai⁴ Xintao Wang^{2†} Zinan Lin⁵
 Xuefei Ning³ Jiwen Yu¹ Pengfei Wan² Yu Wang³ Xihui Liu^{1†}

¹The University of Hong Kong ²Kling Team, Kuaishou Technology ³Tsinghua University
⁴Zhejiang University ⁵Microsoft Research

[Project Page](#)

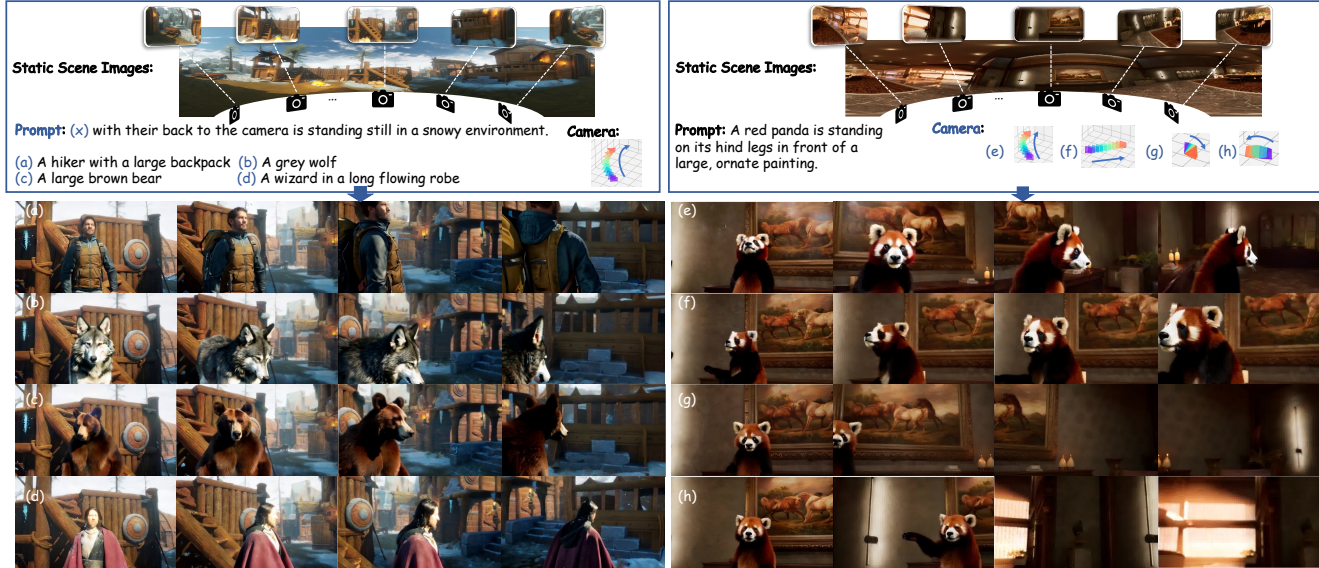


Figure 1. Examples generated by CINESCENE. Given multiple images of a static environment, prompt, and a user-defined camera trajectory, the model generates high-quality videos featuring dynamic subject, while preserving the underlying scene in large view changes.

Abstract

Cinematic video production requires control over scene-subject composition and camera movement, but live-action shooting remains costly due to the need for constructing physical sets. To address this, we introduce the task of cinematic video generation with decoupled scene context: given multiple images of a static environment, the goal is to synthesize high-quality videos featuring dynamic subject while preserving the underlying scene consistency and following a user-specified camera trajectory. We present CINESCENE, a framework that leverages implicit 3D-aware scene representation for cinematic video generation. Our key innovation is a novel context conditioning mechanism that injects 3D-aware features in an implicit way: By encoding scene images into visual representations through VGGT, CINESCENE injects spatial priors into a pretrained text-to-video generation model by addi-

tional context concatenation, enabling camera-controlled video synthesis with consistent scenes and dynamic subjects. To further enhance the model's robustness, we introduce a simple yet effective random-shuffling strategy for the input scene images during training. To address the lack of training data, we construct a scene-decoupled dataset with Unreal Engine 5, containing paired videos of scenes with and without dynamic subjects, panoramic images representing the underlying static scene, along with their camera trajectories. Experiments show that CINESCENE achieves state-of-the-art performance in scene-consistent cinematic video generation, handling large camera movements and demonstrating generalization across diverse environments. Here is the [Project Page](#).

1. Introduction

Cinematic video production requires precise control over scene-subject composition and camera movement [10, 42], making live-action shooting financially and logically de-

*Work done during an internship at Kling Team, Kuaishou Tech.
 †Corresponding author.

manding [49]. In particular, constructing or modifying physical sets for different shots introduces repeated efforts and substantial costs. These challenges highlight the need for a more flexible framework that can create diverse visual narratives without extensive on-set resources. Recent advances in video generation [11, 36, 54] offer a promising avenue to create such a framework. We therefore introduce the task of **cinematic video generation with decoupled scene context**. The goal is to generate a high-quality video featuring a new, dynamic subject based on three inputs: (1) a set of images defining a scene (serving as decoupled scene context), (2) a text prompt, and (3) a user-specified camera trajectory. The generated video must preserve the scene’s consistency across large viewpoint changes while accurately following the desired camera motion, as shown in Figure 1.

Existing approaches for cinematic video generation face a fundamental trade-off between generative flexibility and scene consistency. 2D context-based methods [21, 60] operate directly in image space, offering high flexibility; however, they tend to struggle with maintaining scene consistency when large viewpoint changes occur, due to a lack of spatial understanding. In contrast, 3D-informed methods leverage depth cues [45] or explicit 3D/4D reconstruction [3, 20] to enforce scene consistency. Nevertheless, they tend to be complex and fundamentally limited by the challenge of obtaining accurate 3D/4D representations from sparse inputs [32, 61]. The reliance on imperfect reconstructed geometry often hampers the overall quality of the generated output.

Recent 3D foundation models such as VGGT [56] have demonstrated the ability to obtain comprehensive spatial understanding from 2D images, represented by 3D-aware features. This suggests that robust 3D information can be obtained without resorting to explicit geometric reconstruction. Inspired by this, we propose CINESCENE, a cinematic video generation framework that leverages implicit 3D as scene representation to eliminate the need for explicit geometry. The idea of integrating implicit 3D representations with video diffusion models has been recently explored. For instance, Geometry Forcing [59] combines VGGT with a video diffusion model, using a VGGT-based loss to supervise the generation process. While effective for enforcing consistency, this loss-guided method is fundamentally limited to static scenes without new dynamic subject, as the supervision signal implicitly penalizes dynamic content (Figure 5). *Our key innovation* lies in how we integrate the implicit 3D. Rather than relying on a supervisory loss, CINESCENE introduces a *context conditioning mechanism that directly integrates an implicit 3D scene representation into the video diffusion process*. It enables the model to disentangle the static scene (provided as a conditioning input) from the dynamic content (to be generated), while jointly modeling a decoupled 3D structure and a dynamic

subject. Consequently, our framework overcomes the limitation of prior work [45, 59, 68], which can only generate the static scene without new dynamic content, or are constrained to small view variations. In contrast, our approach generates scene-consistent videos with new dynamic subjects, even under large view changes.

Specifically, we encode static scene images into visual features through VGGT [56], yielding an implicit 3D scene representation that captures both the spatial layout and camera information. These features are then projected and injected into a pretrained text-to-video (T2V) generation model as additional context tokens, allowing the model to preserve scene structure while generating vivid, dynamic content. To further strengthen the alignment between the scene images and their implicit 3D encoding, we introduce a simple but effective random-shuffling strategy for scene images during training. This strategy prevents the model from relying on fixed image ordering and encourages it to learn a robust correspondence between the generated content and the scene context.

Since no existing dataset explicitly separates static environments from dynamic subject, we construct a scene-decoupled dataset using Unreal Engine 5 [17]. This dataset includes videos both with and without dynamic subject, panoramic images representing the underlying static scene, and corresponding camera trajectories. It provides the essential supervision needed to train scene-consistent generative models.

Our contributions are summarized as follows:

- We introduce the task of cinematic video generation with decoupled scene context, enabling scene-consistent dynamic video synthesis in large view changes.
- To the best of our knowledge, we are the first to explore the context conditioning mechanism to inject implicit 3D scene representation that enables video generation models with spatial understanding.
- We construct a scene-decoupled dataset containing panoramas, annotated camera trajectories, and paired videos with/without dynamic subject to enable explicit supervision of scene-consistent video generation with dynamic subject.
- Extensive experiments demonstrate that CINESCENE achieves state-of-the-art performance in cinematic video generation with strong scene consistency and camera accuracy, and exhibits out-of-domain generalization and practical applications in virtual stage production.

2. Related Work

2.1. Video Generation

Video generation has progressed significantly recently, with diffusion model-based [4, 25, 26, 34, 40, 50, 55, 67, 76], and language model-based [8, 9, 37, 53, 69, 70]. Video

diffusion models excel by progressively refining noisy inputs into clean video samples, with recent advancements like Sora [5], HunyuanVideo [38], and Wan-Video [54] demonstrating remarkably high-quality visual synthesis via sophisticated latent diffusion techniques. Video language models, such as VideoPoet [37], are typically derived from the family of transformer-based language models that can flexibly incorporate multiple tasks in pretraining, and show zero-shot capabilities. Recent works [6, 21, 60], such as Veo3 [19], RunwayML [47], and Kling [36] enable high-quality video generation.

2.2. Context Conditioning

Context conditioning paradigm for generation is pioneered in the image domain by OminiControl [52], and then extended to video by FullDiT [24, 31], and LCT [21]. This simple yet effective design allows for flexible conditioning, but with only 2D contexts, it still struggles with the challenge of scene consistency especially under large view changes due to the lack of spatial understanding. Extensive works [58, 62] utilizes a rule-based method to select overlap context images, however, they still need extra camera poses which are not estimated accurately. Recent works [45, 72] inject explicit 3D information (*e.g.*, depth map, point clouds) into video model, however it is complex and hard to get accurate explicit 3D information as guidance. For implicit guidance, prior works [12, 59] investigate methods to enable models to perceive 3D structural information within the diffusion process. FantasyWorld [12] introduces cross-branch supervision, where jointly generates videos and 3D attributes. Geometry Forcing [59] guides video model with 3D loss from VGGT [56]. However, this approach is limited to static scene generation, which restricts its applicability in cinematic video generation involving dynamic content. Different from prior work, we explore the context conditioning mechanism to inject implicit 3D scene representation into a video model for generating novel videos, with no architecture modification. This allows creators to synthesize videos with dynamic content and flexible camera trajectories, all while maintaining scene consistency across large viewpoint changes.

2.3. Cinematic Video Generation

Cinematic video generation aims to incorporate cinematographic principles into both virtual and live-action videos [10, 27, 33]. The Virtual Cinematographer (VC) [23, 65] introduces a paradigm for automatically generating complete camera specifications in real time for capturing events in 3D virtual environments. Other works focus on planning suitable camera placements [13–15, 18, 41, 43] or camera control [1, 22, 66, 74, 75] for interactive tasks. While prior approaches primarily focus on camera setting strategies, our method considers scene consistency,

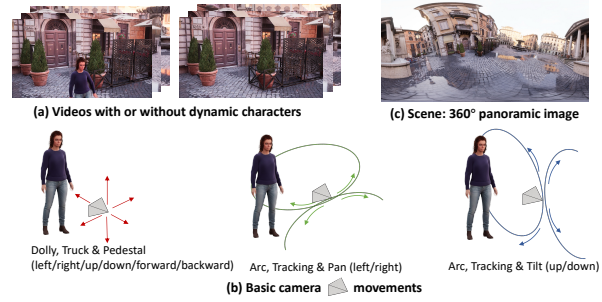


Figure 2. Overview of Scene-Decoupled Video Dataset. For each scene, we render (a) videos with/without dynamic subject, (b) 360° panoramic image representing the static scene from a common starting viewpoint, with (c) diverse camera trajectories.

dynamic content, and camera movements simultaneously, leveraging flexible novel cinematic video generation.

3. Scene-Decoupled Video Dataset

To enable scene-consistent, camera-controlled video generation based on static scene images, data of videos with decoupled scene content and large view changes are required for training the video generation model. Specifically, the data should include videos with dynamic subjects and camera trajectories, paired with static scene images that are shot in the same location. Existing real-world datasets do not readily provide perfectly separated static backgrounds and dynamic foregrounds, nor do they offer the precise and diverse camera trajectory information essential for our task. Therefore, we use a rendering engine Unreal Engine 5 [17] to generate the data. The advantages of this data collection pipeline are: 1) It provides perfectly aligned pairs of dynamic videos and a static representation of the same scene. This perfect pairing is crucial for training a model to learn a decoupled representation of dynamic subjects and the static environment. 2) It enables precise and customizable camera trajectories that support large view changes.

The dataset is shown in Figure 2. For video data, we construct two versions: videos with or without dynamic subject. For the version with dynamic subject, we select randomly the animated human character from our asset library, and place it within multiple 3D environments as in [2]. We randomly combine different characters and their actions in different scenes. For the version without animated characters, we only remove the characters from the scene, leaving others unchanged. For each scene, we define a set of camera trajectories originating from a common starting viewpoint. These trajectories are designed based on fundamental cinematographic movements [42], including “dolly”, “pan”, “tilt”, “tracking” along 6 directions, *i.e.*, up, down, left, right, forward, backward. In order to achieve large view changes, we add constraints to the camera movements, such as 75 degrees for 77 frames in “pan” movement. More details can be found in Appendix. We randomly select a set of trajectories from basic camera movements for each loca-

tion, all of which share a common starting viewpoint. To represent the static scene for each location, we render a full 360-degree panoramic image from the shared starting viewpoint of the video trajectories. This panoramic image is then projected onto an equirectangular representation [28] to represent the static scene, where the horizontal axis represents the longitude and the vertical axis represents the latitude. This format is one of the commonly used for storing 360-degree scene content. In total, we collect 46K video-scene image pairs in 35 high-quality 3D environments with 46K different camera trajectories.

4. Method

Given a set of decoupled scene images $I \in \mathbb{R}^{h \times w \times c}$, a prompt P , and a camera trajectory $C \in \mathbb{R}^{f \times 3 \times 4}$, our objective is to generate a novel video $V \in \mathbb{R}^{f \times c \times h \times w}$ with dynamic subject and specified camera trajectory, where c represents number of channels, h and w are image height and width. V should share the same scene consistency with I . To achieve this, we propose to inject scene images along with their implicit 3D scene representation as conditions via context conditioning into video model. The overview is shown in Figure 3.

4.1. 3D-Aware Scene Representation Extraction

In order to obtain a 3D-aware scene representation, we first get static scene images from the Scene-Decoupled Video Dataset, and then extract the implicit 3D scene representation from these images for subsequent video generation.

Scene Context Images. To simulate the static scene images captured by users, we perform an equirectangular-to-perspective projection [30] based on the panoramic image. Specifically, we generate 20 perspective images from each equirectangular panorama by sampling the viewpoint along the horizontal plane at 18° increments. These decoupled scene images I cover the full 360° horizontal scene. A wide field-of-view (FoV) of 90° is employed to ensure comprehensive scene context is captured in each perspective image.

Implicit 3D Scene Representation. To equip the generation model with the necessary spatial understanding for maintaining scene consistency, we extract implicit 3D scene representation from the static scene images I . Specifically, we leverage the transformer backbone of VGGT [56] to extract features, which has been demonstrated to encode rich spatial information that significantly enhance downstream tasks like point tracking. We obtain the internal features from its final layer. These features are naturally decoupled into two components [56]: the image feature and the camera feature. The image feature $F_i \in \mathbb{R}^{20 \times k \times 2048}$ contains rich spatial cues, including information related to depth maps, point cloud structures, and tracking features. The camera feature $F_c \in \mathbb{R}^{20 \times 1 \times 2048}$, contains camera pose information. To enhance the generation model’s holistic under-

standing of the 3D scene, we construct the final implicit features $F \in \mathbb{R}^{20 \times k \times 2048}$ by incorporating F_i and F_c . k is the number of tokens depending on the resolution. The incorporation is achieved by first expanding F_c to match the spatial dimension of F_i and then performing an element-wise addition. This fusion process effectively combines the scene’s content information F_i with its corresponding camera-viewpoint information F_c , creating a rich implicit representation for the video generation. We found this simple operation to be effective and efficient.

4.2. Video Generation with Decoupled Scene Representation

For video generation, we use scene context images, implicit 3D scene representation, camera, and prompt as inputs. Scene context images and implicit 3D scene representation are projected and injected via context conditioning before transformer blocks.

Scene Context Images Condition. Given scene context images I , CINESCENE uses a causal 3D VAE [35] with temporal compression rate of 4 and spatial compression rate of 8 to encode images. Each image in I ($\in \mathbb{R}^{h \times w \times 3}$) is first encoded to latent $\in \mathbb{R}^{h/8 \times w/8 \times 8}$ with VAE separately, then patchified with a patch size of 2 to get the image token $\in \mathbb{R}^{h/16 \times w/16 \times d}$, where d represents the hidden dimension. Then all the image tokens are concatenated into a sequence in frame dimension as context tokens $I_t \in \mathbb{R}^{20 \times h/16 \times w/16 \times d}$.

Implicit 3D Scene Representaion Condition. The implicit 3D scene is represented as implicit features $F \in \mathbb{R}^{20 \times k \times 2048}$, is first reshaped and interpolated in spatial dimension $\in \mathbb{R}^{20 \times h/8 \times w/8 \times 2048}$ for spatial alignment with I . Then it is patchified and projected to the hidden dimension with a convolutional layer and a layer norm to get implicit 3D tokens $F_t \in \mathbb{R}^{20 \times h/16 \times w/16 \times d}$. The input sequence for the transformer blocks is formed by concatenating the tokens of the noisy video, I_t , and F_t along the frame dimension, allowing jointly modeling of scene images and implicit scene representation.

Camera and Prompt Condition. Unlike previous works [68] that need explicit camera parameters from context images which is challenging to obtain accurate information even with the state-of-the-art structure-from-motion (SfM) methods [2], we only use the desired camera trajectory as input conditions. Given the input camera parameters $C \in \mathbb{R}^{f \times 3 \times 4}$ that include the orientation and translation for each frame, we follow [2] to apply camera injection to facilitate the model in correlating the camera parameters with the generated videos. Specifically, we project C to have the same channels with the video tokens through a learnable camera encoder, and add it into the visual features that correspond to the noisy video. For the visual features that correspond to I_t , and F_t tokens, we inject zero as a place-

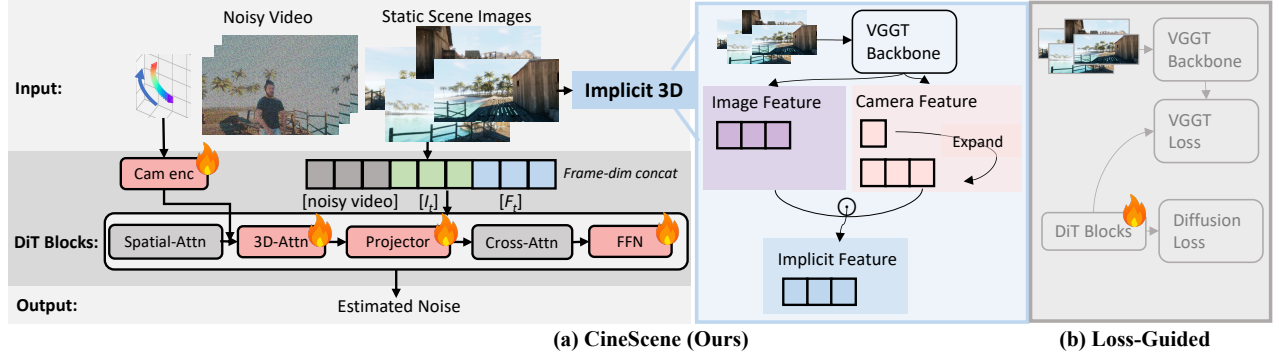


Figure 3. **Overview of CINESCENE.** *Left:* Our method, CINESCENE, injects implicit 3D information as a context condition. Features from VGGT are encoded as tokens (F_t) and concatenated with the scene images (I_t) and the noisy video latents. This architecture fundamentally decouples the static background (the condition) from the dynamic foreground (the generation target). *Right:* In contrast, loss-guided approaches use the VGGT features to form a supervisory loss, which penalizes deviations from the static scene and thus discourages dynamic content generation. We omit the text prompt for simplicity.

holder. We follow [2] not to include camera intrinsics, as users are unlikely to have access to the source images’ intrinsics. For simplicity in our experiments, we maintain a fixed relationship between the FoV of the context images and the generated video. However, our framework can be readily extended to incorporate varying camera intrinsics as an additional input condition with minimal modifications. Then we inject the prompt condition into the cross attention of video model as prior work [46].

Discussion on Context Condition (Ours) v.s. Loss-Guided Method. There has been exploration of integrating implicit 3D information into video diffusion models through a loss-guided mechanism [59]. This approach fine-tunes the video model by minimizing the discrepancy between VGGT features and the diffusion model’s latent representations. While effective, our experimental results demonstrate that our context-conditioning strategy for injecting implicit 3D representations offers substantial advantages over the loss-guided approach, particularly for generating dynamic content (Figure 5). We attribute this superior performance to two key aspects of our method. First, by injecting the scene representation as a context condition rather than as a supervisory loss, our framework inherently decouples the static background from the dynamic foreground. This provides a more robust mechanism for generating vivid motion without being constrained by a loss function optimized for static reconstruction. Second, our approach aligns better with the diffusion paradigm by using VGGT features as guiding context instead of as a separate training objective, unlike the loss-guided method where VGGT supervision and diffusion loss act independently. Our method enables the diffusion model to jointly model the decoupled scene and dynamic subjects.

4.3. Shuffled Context Images Alignment

We observed that using ordered scene context images as inputs for training (which are at equal 18° incremental degrees in the horizontal plane) will dominate the generation

model with pixel information, especially the content of the first and last images (Figure 6). This leads the generation model neglect to learn from the implicit 3D representation. Possible solution includes progressive training strategy [31], that first trains difficult-to-learn part early to ensure the model learn robust representation, and then introduces easier part that benefits from improved feature representation. However, progressive training (train first implicit condition, and then add scene context images) is not suitable for our task, hindering the joint alignment of scene context images and their implicit 3D representation. We attribute this observed issue to position-aware prior introduced by the positional embedding [51] within the video generation model. To mitigate this issue, we propose the context image shuffling mechanism during training. Specifically, we fix the position of the first context image (which corresponds to the starting viewpoint of the target video) in the input sequence, while randomly shuffling the order of the remaining context images. We found that this simple yet effective mechanism enables the generation model to learn the alignment between pixel-level context and implicit 3D scene representation, rather than exploiting correlations from a fixed input order.

5. Experimental Results

5.1. Experimental Settings

Implementation Details. We train CINESCENE based on an internal text-to-video diffusion model with the Scene-Decoupled Video Dataset introduced in Section 3. The model is trained for 10K steps with a batch size of 16, a learning rate of 5×10^{-5} , and a timestep shift of 15. We use 20 scene context images, target camera pose, and target prompt as inputs to the model. For inference, we use a resolution of 384×672 with 77 frames. We set the inference step number as 50.

Baselines. Due to the lack of existing works with the identical experimental setting, we select the follow-

Table 1. **Quantitative comparision with previous methods.** We compare CINESCENE with FramePack [71] on scene consistency, Context-as-Memory [68] and Gen3C [45] on both scene consistency and camera accuracy, Traj-Attn [63] and RecamMaster [2] on camera accuracy. We follow [64] to evaluate video quality on VBench.

Model	Scene Consistency					Camera Accuracy			Text Alignment	Video Quality
	Mat. Pix.(K)↑	CLIP-V↑	PSNR↑	SSIM↑	LPIPS↓	RotErr↓	TransErr↓	CamMC↓	CLIP-T↑	VBench↑
Context-based Method										
FramePack [71]	4107.45	0.8421	11.8854	0.3551	0.5505	-	-	-	0.3269	0.7999
Context-as-Memory [68]	4581.15	0.8542	13.8102	0.3981	0.4486	2.7106	5.2194	6.9554	0.3199	0.8018
Explicit 3D Guidance Method										
Gen3C [45]	4541.25	0.8292	11.6255	0.3125	0.6711	2.9670	10.1578	11.1018	0.2824	0.7585
Camera-Controlled Method										
Traj-Attn [63]	-	-	-	-	-	4.7124	7.8844	11.0607	0.2653	0.7771
ReCamMaster [2]	-	-	-	-	-	3.0854	7.3714	9.2358	0.3086	0.7950
Ours	4617.51	0.8633	14.5094	0.4133	0.4241	2.6825	5.1460	6.8819	<u>0.3212</u>	0.8053

ing methods as baselines for comparison: (1) *Context-based method*: FramePack [71], Context-as-Memory (CaM) [68]. FramePack hierarchically compresses context into frames. Context-as-Memory uses a rule-based FoV selection method, which needs the camera pose of context images. Here we use VGGT [56] to predict camera poses of context images. (2) *Explicit 3D guidance method*: Gen3C [45], conditioning on the 2D renderings of predicted point clouds of images with camera trajectory. (3) *Camera-controlled method*: Trajectory-Attention (Traj-Attn) [63], ReCamMaster [2].

Evaluation. We employ 10 metrics across four key aspects: scene consistency, camera control, text alignment, and overall video quality. (1) *Scene consistency*: we follow prior work [2, 39] to use GIM [48] to calculate the number of matching pixels with confidence greater than the thresholdand (Mean Pixel Error (Mat. Pix.)), and CLIP-V [44] (frame-wise CLIP similarity). We also follow [45] to calculate pixel-align metrics, PSNR and SSIM [57], and perceptual metrics, LPIPS [73]. (2) *Camera accuracy*: we adopt RotErr, TransErr, and CamMC as in CamI2V [74]. (3) *Text alignment*: we use CLIP-T [44], following prior work [2]. (4) *Video quality*: we evaluate on VBench [29] metrics. For test set, due to the lack of existing decoupled scene content data, we follow [68] to randomly choose 300 samples from the held out of the Scene-Decoupled Video Dataset containing scenes with or without dynamic subject for testing. To test the out-of-domain ability, we construct 50 samples from DiT360 [7, 16], which are real-world scenes. We provide OOD qualitative results in Section 5.4, and quantitative results in Appendix.

5.2. Comparison with State-of-the-Art Methods

Quantitative Results. For fair comparison, all context-based methods [68, 71] are reimplemented on our base model and dataset with identical training setting. We employ the T2V model from [2] as its I2V model is not open-source. As show in Table 1, we evaluate scene consistency by comparing CINESCENE against both context-based and explicit 3D guidance methods. The quantitative metrics, in-

cluding Mat. Pix., CLIP-V, PSNR, SSIM, and LPIPS, consistently demonstrate CINESCENE’s superior performance in maintaining scene consistency. This superiority stems from CINESCENE’s effective utilization of joint scene context images coupled with their 3D spatial understanding. FramePack performs poorly in scene consistency due to its reliance on compressed and purely 2D pixel-level scene information. Context-as-Memory struggles with consistency, especially under large view changes, which we attribute to its dependency on both high-overlap context images, and accuracies in estimated camera poses. Gen3C also struggles with scene consistency as it uses explicit 3D guidance, and the inaccuracy of 3D guidance for large view changes causes inconsistency. Furthermore, the method that relies on explicit 3D guidance requires additional inference time, about 10.17× longer than ours. In contrast, our method’s use of implicit 3D information enables it to effectively align the generated video with the underlying 3D structure. Then, we evaluate camera accuracy against methods that are either camera-controlled [2, 63] or use camera parameters as input [45, 68]. The results show that by leveraging implicit 3D information, our method also achieves higher camera accuracy. The text alignment of CINESCENE is slightly lower than that of FramePack since the calculation of text alignment is based on CLIP similarity between frames and the text. As CINESCENE exhibits significantly greater camera movement compared to FramePack, the text alignment metric is impacted by the large change between frames.

Qualitative Results. As illustrated in Figure 4, CINESCENE demonstrates superior scene consistency under large view changes in both dynamic scenes and static scenes, and accuracy in camera control. FramePack can generate novel videos but fails to generate scene-consistent videos with large view changes or limited to a fixed view. Gen3C causes significant scene changes with large view changes, because it relies on the projection of the predicted pixel-wise depth of context images in large view change. When the predicted 3D guidance is not sufficient or accurate, it results in inconsistency. Since context-as-memory and CINESCENE are trained on the same backbone, this

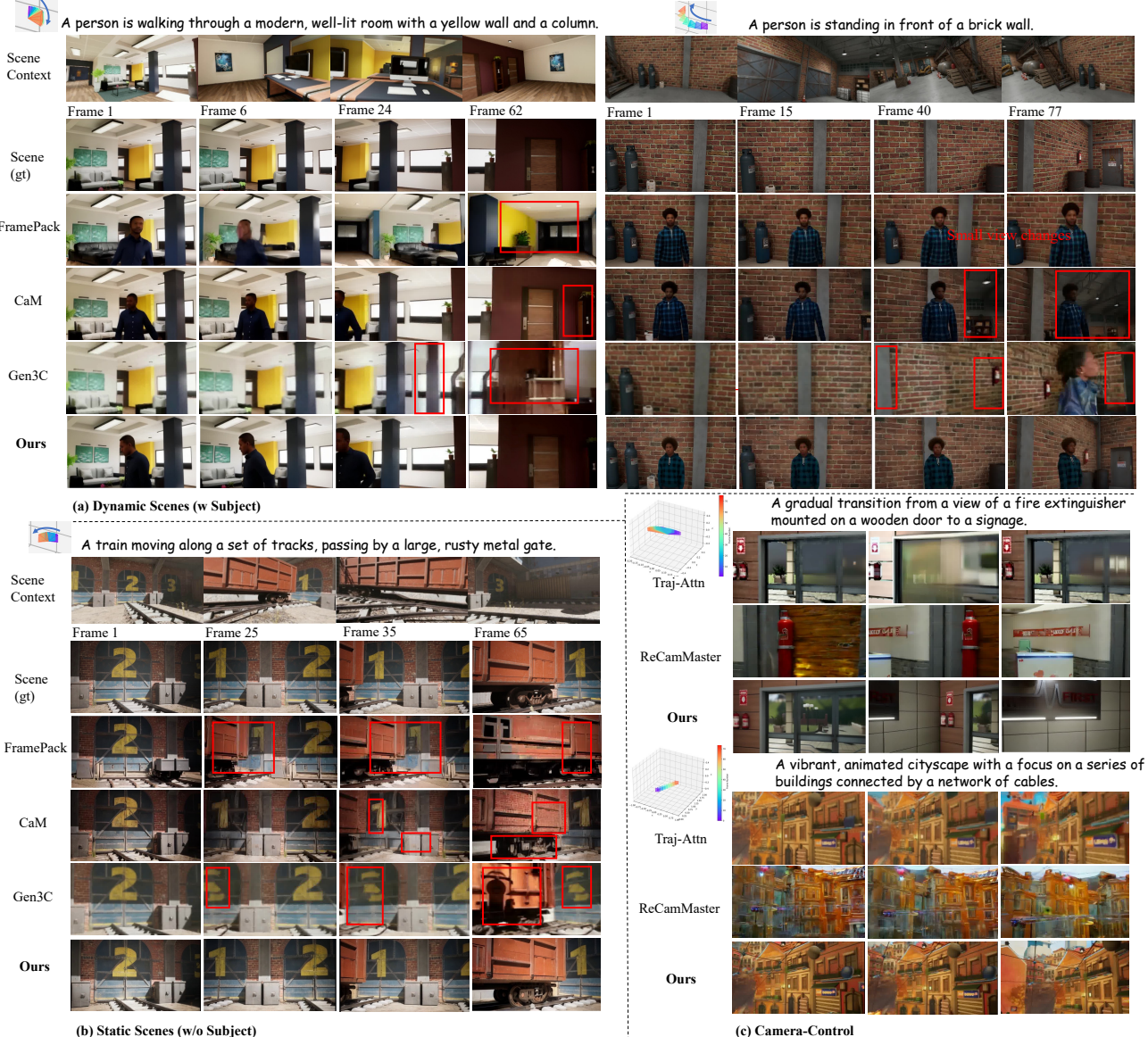


Figure 4. **Qualitative comparison of CINESCENE and previous context-based, explicit 3D guidance, camera-controlled methods.** We present dynamic scenes, static scenes compared with FramePack [71], CaM [68], and Gen3C [45], camera-control with Traj-Attn [63] and RecamMaster [2]. We provide scene ground truth (gt) for comparison. We only show 4 scene context images for illustration.

highlights the effectiveness of scene implicit 3D information injection for scene consistency.

5.3. Ablation Study

Ablation on Different Implicit 3D Methods. We compare our context conditioning (ours) with loss-guided method. The results in Table 2 show that the loss-guided method cause scene inconsistency compared to ours (Loss-Guided v.s. Ours). Also we observed that loss-guided injection method suffer from significant artifacts of dynamic subject due to the penalized loss on dynamic content (Figure 5).

Impact of Scene Implicit 3D Representation. We train four sets of models with different implicit 3D information conditions: (1) without implicit 3D; (2) implicit 3D with



Figure 5. **Qualitative ablation study on injecting implicit 3D methods.** Loss-guided method shows artifacts when generating dynamic subject.

only image feature; (3) implicit 3D with only camera feature; (4) with both image and camera features (ours). We evaluate our model on scene consistency. Results in Table 2 validate our claim that the fusion of scene’s content

Table 2. Ablation on scene implicit 3D representation.

	Mat. Pix.(K)↑	CLIP-V↑	PSNR↑	SSIM↑	LPIPS↓
Loss-Guided	4509.46	0.8552	13.9996	0.4020	0.4458
W/o Implicit	4527.46	0.8456	13.7582	0.3997	0.4506
W/ Image feature	4519.11	0.8518	13.9623	0.3981	0.4474
W/ Camera feature	4498.83	0.8544	14.1058	0.3997	0.4467
Ours	4617.51	0.8633	14.5094	0.4133	0.4241

Table 3. Ablation on shuffled context images.

	Mat. Pix.(K)↑	CLIP-V↑	PSNR↑	SSIM↑	LPIPS↓	RotErr↓	TransErr↓	CamMC↓
Ordered	4673.67	0.8592	14.0174	0.4099	0.4316	2.7329	5.1756	6.9152
Progressive	4531.66	0.8608	14.2008	0.4111	0.4378	2.5757	5.4059	7.0612
Shuffled (Ours)	4617.51	0.8633	14.5094	0.4133	0.4241	2.6825	5.146	6.8819

information and camera-viewpoint information effectively creates a rich and joint representation for video generation in scene consistency.

Impact of Shuffled Context Images. We further analyze the impact of using shuffled mechanism for scene context images. We compare with the ordered scene context images and progressive training described in Section 4.3. We evaluate our model on scene consistency and camera accuracy. Table 3 shows that the shuffled mechanism leads to better joint modeling and learning in scene consistency and camera accuracy. We show the qualitative comparison in Figure 6, that the ordered scene context will let the model copy the content of the last image (marked in red square, copy twice in the generated video), which is inconsistent with the scene, neglecting the learning from implicit 3D.

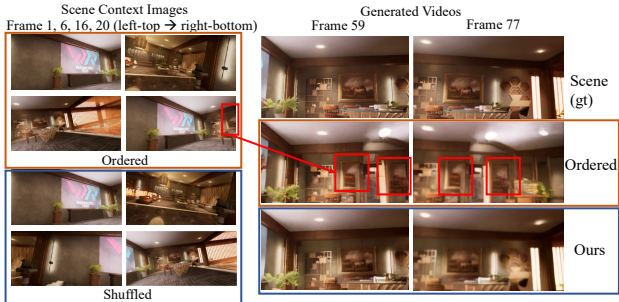


Figure 6. Qualitative ablation study on shuffled context images. The shuffled mechanism leads to better joint modeling and learning in scene consistency, while the ordered ones are tend to copy content from last provided image.

5.4. Applications of CINESCENE

In this section, we show qualitative out-of-domain results in self-constructed samples from DiT360, and show potential applications in cinematic video generation.

Out-of-Domain Results. Shown in Figure 7, our method has the potential to generalize to real-world scenarios.

Application of Virtual Stage. Shown in Figure 8 (first 4 rows), CINESCENE facilitates the creation of diverse performances by different subjects within a consistent virtual environment, streamlining production workflows.

Application of Cinematic Language. Shown in Figure 8 (last two rows), CINESCENE empowers creators to explore diverse camera trajectories for a given performance



Figure 7. Qualitative results of CINESCENE with out-of-domain results. Our method has the potential to generalize to real-world scenarios.

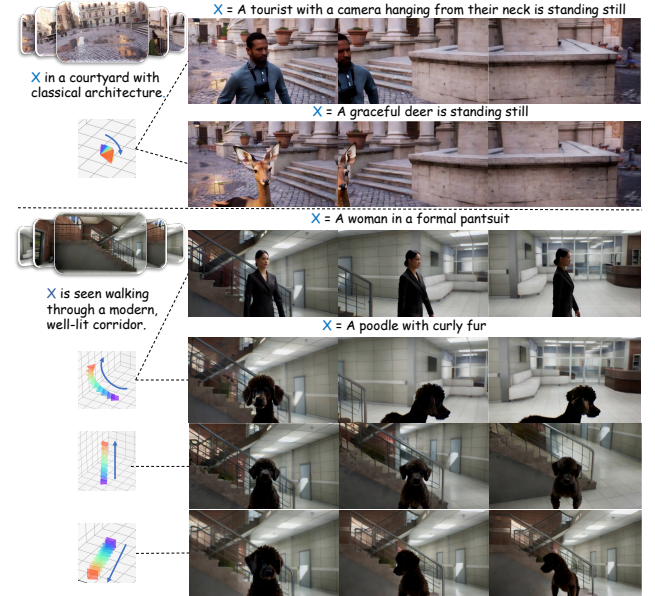


Figure 8. Qualitative results of CINESCENE with diverse scenes, dynamic subjects, and camera trajectories. Our method shows promising application of virtual stage and cinematic language in cinematic video generation.

and static scene, allowing them to shape narrative impact through dynamic camera work, with scene consistency.

6. Conclusion

We present CINESCENE, a cinematic video generation framework that can generate scene-consistent, camera-controlled videos with dynamic subject based on a decoupled scene representation. The method eliminates the need for explicit 3D information while keeping scene consistency in large view changes. We explore the method of injecting implicit 3D-aware scene representation into pretrained T2V model, leveraging its generative capabilities to create dynamic videos. We proposed a simple yet effective shuffling mechanism for the input scene images during both feature extraction and concatenation. Furthermore, we developed a scene-decoupled video dataset using Unreal Engine 5, featuring diverse dynamic content, camera movements, and a variety of static scenes. Extensive experiments demonstrated CINESCENE’s state-of-the-art performance and promising applications.

References

- [1] Sherwin Bahmani, Ivan Skorokhodov, Aliaksandr Siarohin, Willi Menapace, Guocheng Qian, Michael Vasilkovsky, Hsin-Ying Lee, Chaoyang Wang, Jiaxu Zou, Andrea Tagliasacchi, et al. Vd3d: Taming large video diffusion transformers for 3d camera control. *arXiv preprint arXiv:2407.12781*, 2024. 3
- [2] Jianhong Bai, Menghan Xia, Xiao Fu, Xintao Wang, Lianrui Mu, Jinwen Cao, Zuozhu Liu, Haoji Hu, Xiang Bai, Pengfei Wan, et al. Recammaster: Camera-controlled generative rendering from a single video. *arXiv preprint arXiv:2503.11647*, 2025. 3, 4, 5, 6, 7, 1, 2
- [3] Weikang Bian, Zhaoyang Huang, Xiaoyu Shi, Yijin Li, Fu-Yun Wang, and Hongsheng Li. Gs-dit: Advancing video generation with pseudo 4d gaussian fields through efficient dense 3d point tracking. *arXiv preprint arXiv:2501.02690*, 2025. 2
- [4] Andreas Blattmann, Robin Rombach, Huan Ling, Tim Dockhorn, Seung Wook Kim, Sanja Fidler, and Karsten Kreis. Align your latents: High-resolution video synthesis with latent diffusion models. In *Proceedings of the IEEE/CVF Conference on Computer Vision and Pattern Recognition*, pages 22563–22575, 2023. 2
- [5] Tim Brooks, Bill Peebles, Connor Holmes, Will DePue, Yufei Guo, Li Jing, David Schnurr, Joe Taylor, Troy Luhman, Eric Luhman, Clarence Ng, Ricky Wang, and Aditya Ramesh. Video generation models as world simulators. 2024. 3
- [6] Shengqu Cai, Ceyuan Yang, Lvmin Zhang, Yuwei Guo, Junfei Xiao, Ziyan Yang, Yinghao Xu, Zhenheng Yang, Alan Yuille, Leonidas Guibas, et al. Mixture of contexts for long video generation. *arXiv preprint arXiv:2508.21058*, 2025. 3
- [7] Angel Chang, Angela Dai, Thomas Funkhouser, Maciej Halber, Matthias Niessner, Manolis Savva, Shuran Song, Andy Zeng, and Yinda Zhang. Matterport3d: Learning from rgbd data in indoor environments. *International Conference on 3D Vision (3DV)*, 2017. 6, 1
- [8] Huiwen Chang, Han Zhang, Lu Jiang, Ce Liu, and William T Freeman. Maskgit: Masked generative image transformer. In *Proceedings of the IEEE/CVF Conference on Computer Vision and Pattern Recognition*, pages 11315–11325, 2022. 2
- [9] Huiwen Chang, Han Zhang, Jarred Barber, AJ Maschinot, Jose Lezama, Lu Jiang, Ming-Hsuan Yang, Kevin Murphy, William T Freeman, Michael Rubinstein, et al. Muse: Text-to-image generation via masked generative transformers. *arXiv preprint arXiv:2301.00704*, 2023. 2
- [10] David B Christianson, Sean E Anderson, Li-wei He, David H Salesin, Daniel S Weld, and Michael F Cohen. Declarative camera control for automatic cinematography. In *AAAI/IAAI, Vol. 1*, pages 148–155, 1996. 1, 3
- [11] HunyuanVideo Community. Hunyuanvideo: Text-to-video model, 2024. 2
- [12] Yixiang Dai, Fan Jiang, Chiyu Wang, Mu Xu, and Yonggang Qi. Fantasyworld: Geometry-consistent world modeling via unified video and 3d prediction. *arXiv preprint arXiv:2509.21657*, 2025. 3
- [13] Steven Drucker. Intelligent camera control in a virtual environment. 1994. 3
- [14] Steven M Drucker and David Zeltzer. Camdroid: A system for implementing intelligent camera control. In *Proceedings of the 1995 symposium on Interactive 3D graphics*, pages 139–144, 1995.
- [15] Steven M Drucker, Tinsley A Galyean, and David Zeltzer. Cinema: A system for procedural camera movements. In *Proceedings of the 1992 symposium on Interactive 3D graphics*, pages 67–70, 1992. 3
- [16] Haoran Feng, Dizhe Zhang, Xiangtai Li, Bo Du, and Lu Qi. Dit360: High-fidelity panoramic image generation via hybrid training. *arXiv preprint arXiv:2510.11712*, 2025. 6, 1
- [17] Epic Games. Unreal engine 5, 2022. 2, 3
- [18] Michael Gleicher and Andrew Witkin. Through-the-lens camera control. In *Proceedings of the 19th annual conference on Computer graphics and interactive techniques*, pages 331–340, 1992. 3
- [19] Google DeepMind. Veo — google deepmind, 2025. Veo 3 model page. 3
- [20] Zekai Gu, Rui Yan, Jiahao Lu, Peng Li, Zhiyang Dou, Chenyang Si, Zhen Dong, Qifeng Liu, Cheng Lin, Ziwei Liu, et al. Diffusion as shader: 3d-aware video diffusion for versatile video generation control. In *Proceedings of the Special Interest Group on Computer Graphics and Interactive Techniques Conference Papers*, pages 1–12, 2025. 2
- [21] Yuwei Guo, Ceyuan Yang, Ziyan Yang, Zhibei Ma, Zhi-jie Lin, Zhenheng Yang, Dahua Lin, and Lu Jiang. Long context tuning for video generation. *arXiv preprint arXiv:2503.10589*, 2025. 2, 3
- [22] Hao He, Yinghao Xu, Yuwei Guo, Gordon Wetzstein, Bo Dai, Hongsheng Li, and Ceyuan Yang. Cameractrl: Enabling camera control for text-to-video generation. *arXiv preprint arXiv:2404.02101*, 2024. 3
- [23] Li-wei He, Michael F Cohen, and David H Salesin. The virtual cinematographer: A paradigm for automatic real-time camera control and directing. In *Seminal Graphics Papers: Pushing the Boundaries, Volume 2*, pages 707–714. 2023. 3
- [24] Xuanhua He, Quande Liu, Zixuan Ye, Weicai Ye, Qulin Wang, Xiantao Wang, Qifeng Chen, Pengfei Wan, Di Zhang, and Kun Gai. Fulldit2: Efficient in-context conditioning for video diffusion transformers. *arXiv preprint arXiv:2506.04213*, 2025. 3
- [25] Yingqing He, Tianyu Yang, Yong Zhang, Ying Shan, and Qifeng Chen. Latent video diffusion models for high-fidelity long video generation. *arXiv preprint arXiv:2211.13221*, 2022. 2
- [26] Jonathan Ho, William Chan, Chitwan Saharia, Jay Whang, Ruiqi Gao, Alexey Gritsenko, Diederik P Kingma, Ben Poole, Mohammad Norouzi, David J Fleet, et al. Imagen video: High definition video generation with diffusion models. *arXiv preprint arXiv:2210.02303*, 2022. 2
- [27] Kaiyi Huang, Yukun Huang, Xintao Wang, Zinan Lin, Xuefei Ning, Pengfei Wan, Di Zhang, Yu Wang, and Xihui

- Liu. Filmster: Bridging cinematic principles and generative ai for automated film generation. *arXiv preprint arXiv:2506.18899*, 2025. 3
- [28] Yukun Huang, Yanning Zhou, Jianan Wang, Kaiyi Huang, and Xihui Liu. Dreamcube: 3d panorama generation via multi-plane synchronization. *arXiv preprint arXiv:2506.17206*, 2025. 4
- [29] Ziqi Huang, Yinan He, Jiashuo Yu, Fan Zhang, Chenyang Si, Yuming Jiang, Yuanhan Zhang, Tianxing Wu, Qingyang Jin, Nattapol Chanpaisit, et al. Vbench: Comprehensive benchmark suite for video generative models. *arXiv preprint arXiv:2311.17982*, 2023. 6
- [30] Haruya Ishikawa. Pyequilib: Processing equirectangular images with python, 2021. 4
- [31] Xuan Ju, Weicai Ye, Quande Liu, Qiulin Wang, Xintao Wang, Pengfei Wan, Di Zhang, Kun Gai, and Qiang Xu. Fulldit: Multi-task video generative foundation model with full attention. *arXiv preprint arXiv:2503.19907*, 2025. 3, 5
- [32] Nikita Karaev, Ignacio Rocco, Benjamin Graham, Natalia Neverova, Andrea Vedaldi, and Christian Rupprecht. Co-tracker: It is better to track together. In *European conference on computer vision*, pages 18–35. Springer, 2024. 2
- [33] Kaveh Kardan and Henri Casanova. Virtual cinematography of group scenes using hierarchical lines of actions. In *Proceedings of the 2008 ACM SIGGRAPH symposium on Video games*, pages 171–178, 2008. 3
- [34] Levon Khachatryan, Andranik Mojsisyan, Vahram Tadevosyan, Roberto Henschel, Zhangyang Wang, Shant Navasardyan, and Humphrey Shi. Text2video-zero: Text-to-image diffusion models are zero-shot video generators. In *Proceedings of the IEEE/CVF International Conference on Computer Vision*, pages 15954–15964, 2023. 2
- [35] Diederik P Kingma and Max Welling. Auto-encoding variational bayes. *arXiv preprint arXiv:1312.6114*, 2013. 4
- [36] Kling. <https://kling.kuaishou.com/>, 2025. Organization: Kuaishou. 2, 3
- [37] Dan Kondratyuk, Lijun Yu, Xiuye Gu, José Lezama, Jonathan Huang, Rachel Hornung, Hartwig Adam, Hassan Akbari, Yair Alon, Vighnesh Birodkar, et al. Videopoet: A large language model for zero-shot video generation. *arXiv preprint arXiv:2312.14125*, 2023. 2, 3
- [38] Weijie Kong, Qi Tian, Zijian Zhang, Rox Min, Zuozhuo Dai, Jin Zhou, Jiangfeng Xiong, Xin Li, Bo Wu, Jianwei Zhang, Katrina Wu, Qin Lin, Aladdin Wang, Andong Wang, Changlin Li, Duojun Huang, Fang Yang, Hao Tan, Hongmei Wang, Jacob Song, Jiawang Bai, Jianbing Wu, Jinbao Xue, Joey Wang, Junkun Yuan, Kai Wang, Mengyang Liu, Pengyu Li, Shuai Li, Weiyan Wang, Wenqing Yu, Xinchi Deng, Yang Li, Yanxin Long, Yi Chen, Yutao Cui, Yuanbo Peng, Zhentao Yu, Zhiyu He, Zhiyong Xu, Zixiang Zhou, Zunnan Xu, Yangyu Tao, Qinglin Lu, Songtao Liu, Dax Zhou, Hongfa Wang, Yong Yang, Di Wang, Yuhong Liu, Jie Jiang, and Caesar Zhong. Hunyuandideo: A systematic framework for large video generative models, 2024. 3
- [39] Yawen Luo, Jianhong Bai, Xiaoyu Shi, Menghan Xia, Xintao Wang, Pengfei Wan, Di Zhang, Kun Gai, and Tianfan Xue. Camclonemaster: Enabling reference-based camera control for video generation. *arXiv preprint arXiv:2506.03140*, 2025. 6, 3
- [40] Zhengxiong Luo, Dayou Chen, Yingya Zhang, Yan Huang, Liang Wang, Yujun Shen, Deli Zhao, Jingren Zhou, and Tieniu Tan. Videofusion: Decomposed diffusion models for high-quality video generation. In *Proceedings of the IEEE/CVF Conference on Computer Vision and Pattern Recognition*, pages 10209–10218, 2023. 2
- [41] Jock D Mackinlay, Stuart K Card, and George G Robertson. Rapid controlled movement through a virtual 3d workspace. In *Proceedings of the 17th annual conference on Computer graphics and interactive techniques*, pages 171–176, 1990. 3
- [42] Joseph V Mascelli. *The five C's of cinematography*. Grafic Publications Hollywood, 1965. 1, 3
- [43] Cary B Phillips, Norman I Badler, and John Granieri. Automatic viewing control for 3d direct manipulation. In *Proceedings of the 1992 symposium on Interactive 3D graphics*, pages 71–74, 1992. 3
- [44] Alec Radford, Jong Wook Kim, Chris Hallacy, Aditya Ramesh, Gabriel Goh, Sandhini Agarwal, Girish Sastry, Amanda Askell, Pamela Mishkin, Jack Clark, et al. Learning transferable visual models from natural language supervision. In *ICML*, 2021. 6
- [45] Xuanchi Ren, Tianshang Shen, Jiahui Huang, Huan Ling, Yifan Lu, Merlin Nimier-David, Thomas Müller, Alexander Keller, Sanja Fidler, and Jun Gao. Gen3c: 3d-informed world-consistent video generation with precise camera control. In *Proceedings of the Computer Vision and Pattern Recognition Conference*, pages 6121–6132, 2025. 2, 3, 6, 7, 1
- [46] Robin Rombach, Andreas Blattmann, Dominik Lorenz, Patrick Esser, and Björn Ommer. High-resolution image synthesis with latent diffusion models. In *CVPR*, 2022. 5
- [47] Runway AI. Gen-4. <https://runwayml.com/research/introducing-runway-gen-4>, 2025. 3
- [48] Xuelun Shen, Zhipeng Cai, Wei Yin, Matthias Müller, Zijun Li, Kaixuan Wang, Xiaozhi Chen, and Cheng Wang. Gim: Learning generalizable image matcher from internet videos. *arXiv preprint arXiv:2402.11095*, 2024. 6
- [49] Daniel Silva Jasau, Ana Martí-Testón, Adolfo Muñoz, Flavio Moriniello, J Ernesto Solanes, and Luis Gracia. Virtual production: Real-time rendering pipelines for indie studios and the potential in different scenarios. *Applied Sciences*, 14(6):2530, 2024. 2
- [50] Uriel Singer, Adam Polyak, Thomas Hayes, Xi Yin, Jie An, Songyang Zhang, Qiyuan Hu, Harry Yang, Oron Ashual, Oran Gafni, et al. Make-a-video: Text-to-video generation without text-video data. *arXiv preprint arXiv:2209.14792*, 2022. 2
- [51] Jianlin Su, Murtadha Ahmed, Yu Lu, Shengfeng Pan, Wen Bo, and Yunfeng Liu. Roformer: Enhanced transformer with rotary position embedding. *Neurocomputing*, 568:127063, 2024. 5
- [52] Zhenxiong Tan, Songhua Liu, Xingyi Yang, Qiaochu Xue, and Xinchao Wang. Ominicontrol: Minimal and universal control for diffusion transformer. In *Proceedings of the IEEE/CVF International Conference on Computer Vision*, pages 14940–14950, 2025. 3

- [53] Ruben Villegas, Mohammad Babaizadeh, Pieter-Jan Kindermans, Hernan Moraldo, Han Zhang, Mohammad Taghi Saffar, Santiago Castro, Julius Kunze, and Dumitru Erhan. Phenaki: Variable length video generation from open domain textual descriptions. In *International Conference on Learning Representations*, 2022. 2
- [54] Ang Wang, Baole Ai, Bin Wen, Chaojie Mao, Chen-Wei Xie, Di Chen, Feiwu Yu, Haiming Zhao, Jianxiao Yang, Jianyuan Zeng, Jiayu Wang, Jingfeng Zhang, Jingren Zhou, Jinkai Wang, Jixuan Chen, Kai Zhu, Kang Zhao, Keyu Yan, Lianghua Huang, Mengyang Feng, Ningyi Zhang, Pandeng Li, Pingyu Wu, Ruihang Chu, Ruili Feng, Shiwei Zhang, Siyang Sun, Tao Fang, Tianxing Wang, Tianyi Gui, Tingyu Weng, Tong Shen, Wei Lin, Wei Wang, Wei Wang, Wenmeng Zhou, Wente Wang, Wenting Shen, Wenyuan Yu, Xianzhong Shi, Xiaoming Huang, Xin Xu, Yan Kou, Yangyu Lv, Yifei Li, Yijing Liu, Yiming Wang, Yingya Zhang, Yitong Huang, Yong Li, You Wu, Yu Liu, Yulin Pan, Yun Zheng, Yuntao Hong, Yupeng Shi, Yutong Feng, Zeyinzi Jiang, Zhen Han, Zhi-Fan Wu, and Ziyu Liu. Wan: Open and advanced large-scale video generative models. *arXiv preprint arXiv:2503.20314*, 2025. 2, 3
- [55] Juniu Wang, Hangjie Yuan, Dayou Chen, Yingya Zhang, Xiang Wang, and Shiwei Zhang. Modelscope text-to-video technical report. *arXiv preprint arXiv:2308.06571*, 2023. 2
- [56] Jianyuan Wang, Minghao Chen, Nikita Karaev, Andrea Vedaldi, Christian Rupprecht, and David Novotny. Vggt: Visual geometry grounded transformer. In *Proceedings of the Computer Vision and Pattern Recognition Conference*, pages 5294–5306, 2025. 2, 3, 4, 6
- [57] Zhou Wang, Alan C Bovik, Hamid R Sheikh, and Eero P Simoncelli. Image quality assessment: from error visibility to structural similarity. *IEEE transactions on image processing*, 13(4):600–612, 2004. 6
- [58] Zhendong Wang, Yifan Jiang, Yadong Lu, Yelong Shen, Pengcheng He, Weizhu Chen, Zhangyang Wang, and Mingyuan Zhou. In-context learning unlocked for diffusion models, 2023. 3
- [59] Haoyu Wu, Diankun Wu, Tianyu He, Junliang Guo, Yang Ye, Yueqi Duan, and Jiang Bian. Geometry forcing: Marrying video diffusion and 3d representation for consistent world modeling. *arXiv preprint arXiv:2507.07982*, 2025. 2, 3, 5
- [60] Junfei Xiao, Ceyuan Yang, Lvmi Zhang, Shengqu Cai, Yang Zhao, Yuwei Guo, Gordon Wetzstein, Maneesh Agrawala, Alan Yuille, and Lu Jiang. Captain cinema: Towards short movie generation. *arXiv preprint arXiv:2507.18634*, 2025. 2, 3
- [61] Yuxi Xiao, Qianqian Wang, Shangzhan Zhang, Nan Xue, Sida Peng, Yujun Shen, and Xiaowei Zhou. Spatialtracker: Tracking any 2d pixels in 3d space. In *Proceedings of the IEEE/CVF Conference on Computer Vision and Pattern Recognition*, pages 20406–20417, 2024. 2
- [62] Zeqi Xiao, Yushi Lan, Yifan Zhou, Wenqi Ouyang, Shuai Yang, Yanhong Zeng, and Xingang Pan. Worldmem: Long-term consistent world simulation with memory. *arXiv preprint arXiv:2504.12369*, 2025. 3
- [63] Zeqi Xiao, Wenqi Ouyang, Yifan Zhou, Shuai Yang, Lei Yang, Jianlou Si, and Xingang Pan. Trajectory attention for fine-grained video motion control. In *The Thirteenth International Conference on Learning Representations*, 2025. 6, 7, 1, 2, 3
- [64] Liangbin Xie, Yu Li, Shian Du, Menghan Xia, Xintao Wang, Fanghua Yu, Ziyan Chen, Pengfei Wan, Jiantao Zhou, and Chao Dong. Simplegvr: A simple baseline for latent-cascaded video super-resolution. *arXiv preprint arXiv:2506.19838*, 2025. 6, 2
- [65] Zhenran Xu, Longyue Wang, Jifang Wang, Zhouyi Li, Senbao Shi, Xue Yang, Yiyu Wang, Baotian Hu, Jun Yu, and Min Zhang. Filmagent: A multi-agent framework for end-to-end film automation in virtual 3d spaces. *arXiv preprint arXiv:2501.12909*, 2025. 3
- [66] Shiyuan Yang, Liang Hou, Haibin Huang, Chongyang Ma, Pengfei Wan, Di Zhang, Xiaodong Chen, and Jing Liao. Direct-a-video: Customized video generation with user-directed camera movement and object motion. In *ACM SIGGRAPH 2024 Conference Papers*, pages 1–12, 2024. 3
- [67] Zhuoyi Yang, Jiayan Teng, Wendi Zheng, Ming Ding, Shiyu Huang, Jiazhen Xu, Yuanming Yang, Wenyi Hong, Xiaohan Zhang, Guanyu Feng, et al. Cogvideox: Text-to-video diffusion models with an expert transformer. *arXiv preprint arXiv:2408.06072*, 2024. 2
- [68] Jiwen Yu, Jianhong Bai, Yiran Qin, Quande Liu, Xintao Wang, Pengfei Wan, Di Zhang, and Xihui Liu. Context as memory: Scene-consistent interactive long video generation with memory retrieval. *arXiv preprint arXiv:2506.03141*, 2025. 2, 4, 6, 7
- [69] Lijun Yu, Yong Cheng, Kihyuk Sohn, José Lezama, Han Zhang, Huiwen Chang, Alexander G Hauptmann, Ming-Hsuan Yang, Yuan Hao, Irfan Essa, et al. Magvit: Masked generative video transformer. In *Proceedings of the IEEE/CVF Conference on Computer Vision and Pattern Recognition*, pages 10459–10469, 2023. 2
- [70] Lijun Yu, José Lezama, Nitesh B Gundavarapu, Luca Verhari, Kihyuk Sohn, David Minnen, Yong Cheng, Agrim Gupta, Xiuye Gu, Alexander G Hauptmann, et al. Language model beats diffusion–tokenizer is key to visual generation. *arXiv preprint arXiv:2310.05737*, 2023. 2
- [71] Lvmi Zhang and Maneesh Agrawala. Packing input frame context in next-frame prediction models for video generation. *arXiv preprint arXiv:2504.12626*, 2025. 6, 7, 2
- [72] Qihang Zhang, Shuangfei Zhai, Miguel Angel Bautista Martin, Kevin Miao, Alexander Toshev, Joshua Susskind, and Jiatao Gu. World-consistent video diffusion with explicit 3d modeling. In *Proceedings of the Computer Vision and Pattern Recognition Conference*, pages 21685–21695, 2025. 3
- [73] Richard Zhang, Phillip Isola, Alexei A Efros, Eli Shechtman, and Oliver Wang. The unreasonable effectiveness of deep features as a perceptual metric. In *Proceedings of the IEEE conference on computer vision and pattern recognition*, pages 586–595, 2018. 6
- [74] Guangcong Zheng, Teng Li, Rui Jiang, Yehao Lu, Tao Wu, and Xi Li. Cami2v: Camera-controlled image-to-video diffusion model. *arXiv preprint arXiv:2410.15957*, 2024. 3, 6
- [75] Sixiao Zheng, Zimian Peng, Yanpeng Zhou, Yi Zhu, Hang Xu, Xiangru Huang, and Yanwei Fu. Vidcraft3: Camera,

- object, and lighting control for image-to-video generation.
arXiv preprint arXiv:2502.07531, 2025. 3
- [76] Daquan Zhou, Weimin Wang, Hanshu Yan, Weiwei Lv, Yizhe Zhu, and Jiashi Feng. Magicvideo: Efficient video generation with latent diffusion models. *arXiv preprint arXiv:2211.11018*, 2022. 2
- [77] Tinghui Zhou, Richard Tucker, John Flynn, Graham Fyffe, and Noah Snavely. Stereo magnification: Learning view synthesis using multiplane images. *arXiv preprint arXiv:1805.09817*, 2018. 3

CINESCENE: Implicit 3D as Effective Scene Representation for Cinematic Video Generation

Supplementary Material

A. Dataset Construction

We follow [2] to use Unreal Engine 5 to construct Scene-Decoupled Video Dataset as described in Section 3.

3D Environments. We collect 35 different 3D environment assets from [here](#). We mitigate the domain shift from rendered data to real-world distributions by prioritizing high-fidelity 3D assets while incorporating surreal environments as an auxiliary. Environmental variety is achieved through a diverse selection of internal and external venues, ranging from metropolitan streets and commercial interiors to pastoral settings.

Subjects. We collect 70 different human 3D models as subjects from [source A](#) and [source B](#), covering a wide range of styles such as realistic, anime, game-style.

Animations. We collect around 100 different animations from [source A](#) and [source B](#), including diverse dynamic animations (*e.g.*, waving, dancing, cheering).

Camera Trajectories In order to achieve large view changes, we add constraints to the camera movements. The speed of camera movements is set to be linear.

1. **Arc Movements (Left/Right):** For “arc” movements, the camera traverses an arc spanning 75 degrees over 77 frames, continuously tracking the dynamic subject to ensure it remains in view.
2. **Pan Movements (Left/Right):** For “pan” movements, we require a 75-degree rotation over 77 frames. This movement involves only camera rotation, with no change in its spatial position.
3. **Arc and Tilt Movements (Up/Down):** The vertical camera motion is constrained between 10 and 45 degrees relative to its initial orientation. For “arc” movements, the camera tracks the dynamic subject. For “tilt” movements, the camera only rotates with no change in translation.
4. **Dolly, Truck, and Pedestal Movements (Left/Right/Up/Down/Forward/Backward):** For dolly, truck, and pedestal movements, we randomly select the distance thresholds relative to the dynamic subject. The specific ranges for these movements are defined as follows:
 - Left: [1/4, 2]
 - Right: [1/4, 2]
 - Forward: [1/4, 5/4]
 - Backward: [1/4, 2]
 - Up: [1/4, 2/3]
 - Down: [1/4, 2/3]

These values represent the relative distance changes with

respect to the subject.

Initial Viewpoint: The starting viewpoint for all camera movements and the panoramic images is randomly selected within a range of -45 to 45 degrees. This angle is measured relative to the front-facing direction of the dynamic subject, introducing variability in initial perspectives.

B. Implementation Details

Our model’s trainable components include: 1) the 3D attention, projector, and feedforward layers within the DiT Blocks; 2) a convolutional layer and a Layer Normalization module for projecting the implicit 3D features; and 3) a learnable camera encoder for projecting the camera condition [2]. For the baselines compared [2, 45, 63], we utilize the default parameters (*e.g.*, number of generated frames) provided in their official GitHub repositories to ensure a fair evaluation of their standard performance.

C. Experimental Results

C.1. Out-of-Domain Test

To evaluate the model’s generalization capabilities, we conduct an out-of-domain (OOD) test using the DiT360 dataset [7, 16]. This section first explains the construction of our test set and then presents the quantitative and qualitative results.

OOD Test Set Construction. The DiT360 dataset [7, 16] comprises static panoramic views stitched from RGB-D images of building-scale scenes. From this dataset, we selected 50 panoramic images as our test samples. Since each panorama originates from a single viewpoint, we are limited to “pan” camera trajectories, which involve only rotational movements without any translation. To construct the test set, we process each panoramic image in two ways: 1) We project the panorama into a series of context images by sampling viewpoints along the horizontal plane at 18° increments; 2) We define three distinct camera trajectories to generate the ground truth sequences. It is important to note that this test set exclusively contains static scenes. Consequently, this evaluation focuses on comparing the methods’ abilities to generate coherent and consistent static environments.

Quantitative Results on OOD Test Set.

The quantitative results are presented in Table 4. Our proposed method demonstrates superior performance in scene consistency, as evidenced by its leading scores across the Mat. Pix., PSNR, SSIM, and LPIPS metrics. Furthermore, our model achieves the second-highest CLIP-V score.

Table 4. **Quantitative comparision with previous methods on OOD test set.** We compare CINESCENE with FramePack [71] on scene consistency, Context-as-Memory [68] and Gen3C [45] on both scene consistency and camera accuracy, Traj-Attn [63] and RecamMaster [2] on camera accuracy. We follow [64] to evaluate video quality on Vbench.

Model	Scene Consistency					Camera Accuracy			Text Alignment	Video Quality
	Mat. Pix.(K)↑	CLIP-V↑	PSNR↑	SSIM↑	LPIPS↓	RotErr↓	TransErr↓	CamMC↓	CLIP-T↑	VBench↑
Context-based Method										
FramePack [71]	4025.98	0.8784	9.9902	0.3529	0.6625	-	-	-	0.3223	0.7813
Context-as-Memory [68]	4338.75	0.8976	10.1676	0.364	0.6698	5.5482	11.2567	14.0722	0.3112	0.8093
Explicit 3D Guidance Method										
Gen3C [45]	4246.33	0.9049	11.9062	0.4412	0.6309	4.2975	10.8731	13.1951	0.3004	0.738
Camera-Controlled Method										
Traj-Attn [63]	-	-	-	-	-	4.3117	13.2458	14.899	0.3072	0.7635
RecamMaster [2]	-	-	-	-	-	3.7125	11.3909	13.0711	0.3052	0.7705
Ours	4726.57	0.9038	12.0215	0.4470	0.5121	3.6981	10.8435	12.3307	0.3025	0.7965

Table 5. **Ablation study on number of scene context images.**

# Num	Scene Consistency					Camera Accuracy		
	Mat. Pix. (K)↑	CLIP-V↑	PSNR↑	SSIM↑	LPIPS↓	RotErr↓	TransErr↓	CamMC↓
1	3614.14	0.7876	10.3426	0.1682	0.6478	3.9551	8.7780	10.8669
4	4200.82	0.8167	10.7466	0.2215	0.6069	2.3948	7.7557	8.9438
10	4519.10	0.8389	11.9169	0.2890	0.5447	3.0033	7.9496	9.5312
20	4617.51	0.8633	14.5094	0.4133	0.4241	2.6825	5.1460	6.8819

Table 6. **Ablation on camera control condition.**

	RotErr↓	TransErr↓	CamMC↓
W/o Implicit	2.7362	5.4411	7.1805
W/o Camera	11.3678	11.1976	19.5482
Ours	2.6825	5.146	6.8819

In terms of camera accuracy, the RotErr, TransErr, and CamMC metrics confirm the effectiveness of our method.

Qualitative Results on OOD Test Set. Please see the qualitative results in the supplementary video.

C.2. Ablation Study

Ablation on Number of Scene Context Images.

We conduct four experiments on different numbers of scene context images: 1, 4, 10, and 20. The results are shown in Table 5. The results show that increasing the number of scene context images leads to a consistent improvement in performance across both scene consistency and camera accuracy. For scene consistency, all metrics show a clear positive trend. As the number of views increases from 1 to 20, the Mat. Pix. and CLIP-V scores steadily rise, while the LPIPS error consistently decreases. This demonstrates that more contextual information helps the model generate scenes with higher geometric fidelity and semantic coherence. PSNR and SSIM, show a marked increase, signifying a substantial enhancement in the clarity and structural integrity of the generated videos. For camera accuracy, the overall trend also confirms the benefit of us-

ing more views, with the 20-view configuration achieving the lowest error rates across RotErr, TransErr, and CamMC. We observe a slight, non-monotonic degradation in performance when moving from 4 to 10 views. This might suggest that a moderate number of views can introduce temporary ambiguities for camera pose estimation, which are effectively resolved when a richer set of 20 views provides more robust constraints.

Impact of Camera Control. We conduct three experiments on camera accuracy: (1) without implicit 3D information, with camera condition; (2) with implicit 3D information, without camera condition; (3) with both (ours). Results in Table 6 show that the input camera instruction provides fine-grained and accurate control, while implicit 3D information further boosts the camera control.

Different Condition Mechanisms. We show the results in Table 8. (1) Different concatenations. We ablate injecting conditions on channel/view-dimension [2]. We found that frame-dimension (ours) provides a more robust way for the spatio-temporal interactions among conditions, which is also observed in [2]. (2) Different Fusion Strategies. We compare ours with concatenating F_i and F_c directly into tokens without element-wise addition. Our fusion strategy better integrates scene content and viewpoints, enhancing consistency. (3) The camera accuracy are on par among the different mechanisms, as it is mainly impacted by injecting camera trajectory (also validated in Table 6 and Table 9).

Inconsistent Modalities. We evaluate robustness by removing scene descriptions or using inconsistent prompts

Table 7. Ablation study on scene descriptions.

Method	Scene Consistency					Camera Accuracy			Text Alignment	Video Quality
	Mat. Pix.(K)↑	CLIP-V↑	PSNR↑	SSIM↑	LPIPS↓	RotErr↓	TransErr↓	CamMC↓	CLIP-T↑	VBench ↑
remove scene description	4589.18	0.8576	14.3361	0.4159	0.4293	2.4974	5.3	6.8412	0.3057	0.8022
add inconsistent description	4577.54	0.8547	14.2669	0.4103	0.4308	2.474	5.2749	6.7745	0.3048	0.8006
Ours	4617.51	0.8633	14.5094	0.4133	0.4241	2.6825	5.146	6.8819	0.3212	0.8053

Table 8. Ablation study on different feature fusion strategies.

Method	Scene Consistency					Camera Accuracy			Text Alignment	Video Quality
	Mat. Pix.(K)↑	CLIP-V↑	PSNR↑	SSIM↑	LPIPS↓	RotErr↓	TransErr↓	CamMC↓	CLIP-T↑	VBench ↑
channel-dim	4564.53	0.8301	14.0434	0.4024	0.4372	2.4813	5.0500	6.6230	0.3170	0.8041
view-dim	4407.87	0.8265	12.8336	0.3757	0.4974	2.4915	5.9913	7.4144	0.3213	0.7982
separate F_i, F_c	4546.81	0.8533	14.1516	0.4037	0.4449	2.7345	5.4331	7.1764	0.3229	0.8022
Ours	4617.51	0.8633	14.5094	0.4133	0.4241	2.6825	5.1460	6.8819	0.3212	0.8053

Table 9. Ablation on camera control condition. Supplement to Table 2

	RotErr↓	TransErr↓	CamMC↓
w/o Implicit	2.7362	5.4411	7.1805
w/ Image feature	2.4967	5.2081	6.7754
w/ Camera feature	2.7631	5.1620	6.9542
w Implicit (Ours)	2.6825	5.146	6.8819

Table 10. Ablation on OOD trajectories.

Method	Camera Accuracy			Text Alignment	Video Quality
	RotErr↓	TransErr↓	CamMC↓	CLIP-T↑	VBench↑
ReCamMaster [2]	2.2485	7.4892	8.5504	0.3051	0.8015
Traj-Attn [63]	3.4825	8.6681	10.5595	0.2669	0.7728
Ours	2.4147	6.7794	8.0997	0.3163	0.8022

(e.g., “in the garden”). Despite a slight performance drop, our method remains robust to missing or mismatched descriptions, shown in Table 7.

Out-of-range trajectories. Following [39], we evaluate 300 unseen trajectories from RealEstate10K [77]. As ground truth videos are lack for consistency evaluation, we report all other available metrics in Table 10. Our model shows generalization to out-of-range trajectories, benefiting from the 46K diverse trajectories in our dataset.

C.3. More Qualitative Results

Please refer to our [project page](#).

D. Limitations

Our current work presents several limitations that motivate future research directions:

1) We explore the generation of short video clips (77 frames) with a maximum view change of 75 degrees. Extending scene consistency to longer videos with larger view

changes remains a challenging but important area for future investigation.

2) To simplify the problem, we provide the first scene context image with the same viewpoint as the first frame of the generated video. Future work will address the generation of videos from random camera positions.

3) CINESCENE inherits limitations from the pre-trained T2V models, such as distortion in humans’ large motion movements.